ELSEVIER

Journal of Photochemistry and Photobiology
A: Chemistry 85 (1995) 77–83

Journal of
PHOTOCHEMISTRY
AND
PHOTOBIOLOGY
A:CHEMISTRY

Electron transfer and magnetic field effects in covalently linked pyrenyl–oligopeptide–dimethylaniline compounds

Udo Werner, Alexander Wiessner, Wolfgang Kühnle, Hubert Staerk *

Max-Planck-Institut für Biophysikalische Chemie, Abteilung Spektroskopie und Photochemische Kinetik, Am Fassberg, D-37077 Göttingen, Germany

Received 25 March 1994; accepted 7 June 1994

Abstract

The influence of external magnetic fields on the spin dynamics and recombination reaction yield of radical ion pairs, generated by photoinduced electron transfer between pyrenyl and dimethylaniline linked by an oligopeptide bridge, was studied. From the size and characteristics of the magnetic field effect (MFE), it can be concluded that hydrogen bonds within short peptide chains (here three glycine groups) or with a hydrogen-accepting solvent (acetone) do not seem to affect significantly the chain dynamics.

Keywords: Electron transfer; Magnetic field effects; Spin dynamics; Recombination reaction

1. Introduction

Intramolecular photoinduced electron transfer (PET) reactions, in which electron transfer occurs between donor (D) and acceptor (A) sites separated by a synthetic peptide or protein fragment, with A or D in the excited state, have provided insight into the role of the peptide and protein in the control and mediation of through-space or through-bond electron transfer [1]. Different types of bridge structure have been synthesized and the influence of parameters, such as the length or rigidity of the bridge, have been reported. The motivation for PET investigations of peptide-linked molecules comes from different sources:

(1) biological PET is thought to occur at least in part along peptide chains;

(2) peptide chains allow a wide variation of chain properties which determine the shape of the A–D distance distribution as well as its dynamics;

(3) peptide chain conformations are a topic of great biological relevance; in addition, most enzymes are composed of peptide chains whose functions are essentially determined by their steric structure.

Several research groups have been engaged in PET studies of peptide-linked A–D systems for some considerable time. Isied and coworkers initially investigated different types of peptide chain [2] and later concentrated mainly on proline chains [3]. Within the class of peptides, proline occupies a special position; instead of a side-chain it features a five-membered ring at the central carbon atom which makes the peptide more rigid. Oligoproline chains are considered to be rigid by these workers and allow an investigation to be made of the distance dependence of ET without considering the chain dynamics [1]. Schanze and Sauer [4] also investigated the distance dependence of ET with proline chains of varying length. Liu et al. [5] explored a model system for the photosynthetic reaction center, where a porphyrin is covalently linked via short peptide bridges to a quinone. Information has been gathered on the role of through-bond and through-space contributions to ET, in particular on the role of superexchange. Possible pathways for electron tunneling through a saturated chain are reported in Ref. [6]. Contrary to the general opinion that an essential part of ET proceeds by a through-bond mechanism [3,5,7], Inai et al. [8] found an indication for pure through-space ET in a helical peptide molecule.

Investigations of peptide-linked molecules by examination of the magnetic field effect (MFE) on the reaction yield of recombining radical ions have not been carried out to our knowledge. The interplay of the different parameters, which bring about and influence the appearance of the MFE, will not be repeated

* Corresponding author.

SSDI 1010-6030(94)03902-7

here since a number of review articles on this subject have been published, e.g. Ref. [9]. A schematic description outlining the main steps of the MFE mechanism and the different contributions to the spin dynamics has been given recently [10]. Of particular importance are the distribution function of the radical pair distances (see also Ref. [11]) and the dynamics of the changes in molecular conformation leading to changes in the relative intramolecular distance between radical pairs and thus to a complicated influence on the distribution function of the exchange interaction J (because $J(r, t)$ is a function of the distance of the unpaired electron spins and a function of time [10,12]).

A suggestion, which is contrary to accepted ideas on the role of intramolecular hydrogen bonds in protein structures, has been discussed by Ruttens et al. [13]. It is proposed that due to intramolecular hydrogen bonds, a glycine chain may exist predominantly in its maximally extended conformation. This conclusion has been drawn by these workers from the fluorescence yields of exciplexes formed by pyrene and indole, tethered to peptide chains. The main concern of the present work is to study the dynamics of short oligopeptide chains by making use of the MFE, which is sensitive to the relative motions of chain-linked radicals [10]. Any significant influence of intramolecular hydrogen bonds on the chain dynamics should be reflected in the shape and characteristics of the MFE spectra. A comparison is made with the dynamics of polymethylene chains.

Fig. 1 shows the structures of the compounds investigated. The chain of pyrene$(Pt)_3$DMA is designated as $(Pt)_3$, although strictly speaking only the central $CO-CH_2-NH$ portions are complete parts of the glycine peptide. Furthermore, an additional CH_2 group is incorporated between the carbonyl group and DMA in order to prevent direct electronic interaction between the aromatic ring and the carbonyl group. The chain $(Pt)_3$ thus features ten atoms in the linkage between the functional end groups pyrene and DMA. Its fully extended length falls between that of a $(CH_2)_9$ and a $(CH_2)_{10}$ chain. Molecules in which pyrene and DMA are linked by a polymethylene chain are designated in this work as Py(n)DMA, where n is the number of CH_2 groups. The $(Pt)_1$ chain corresponds to the chain in Py(4)DMA. Two different configurations of the $(Pt)_3$-linked molecules were investigated, with pyrene attached at the 1-position (1Py$(Pt)_3$DMA) or at the 2-position (2Py$(Pt)_3$DMA), as indicated in Fig. 1. Similar designations are used with polymethylene-linked molecules.

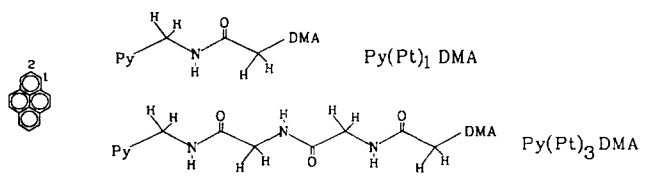

Fig. 1. Structures of the investigated peptide-linked molecules 1Py$(Pt)_1$DMA, 1Py$(Pt)_3$DMA and 2Py$(Pt)_3$DMA (DMA, dimethylaniline; Py, pyrene).

The general reaction scheme for flexibly linked A–D systems in a highly polar solvent is presented in Fig. 2. After excitation of the acceptor molecule A, electron transfer from ^1D to $^1A^*$ generates the radical ion pair (RIP) in its overall singlet state, $^1(^2A^- - ^2D^+)$. The elementary step of RIP formation by electron transfer, as well as the process of RIP recombination by return electron transfer, takes place with overall electron spin conservation. For our system, this results in definite spin selection rules for RIP recombination: singlet pairs yield recombination products in the singlet (ground) state or singlet exciplexes, while triplet pairs yield the triplet excited state. The formation of the RIP in its overall triplet state $^3(^2A^- - ^2D^+)$, with a rate designated by $k_{st}(B)$, requires spin realignment in the pair. This is brought about by the hyperfine-coupling-induced (hfc-induced) coherent spin motion of the unpaired electron spins and can be modulated by weak magnetic fields of strength B by virtue of the Zeeman effect and by the varying exchange interaction. Thus the relative fractions of singlet ground state and triplet excited state products, as well as contact ion pairs which are emissive exciplexes (cf. Fig. 2), can be sensitively influenced by controlling the exchange interaction and by applying an external magnetic field.

2. Experimental section

Steady state fluorescence spectra were measured with a commercial luminescence spectrometer (LS50, Perkin–Elmer). Fig. 3 shows the spectrum of the strongly quenched pyrenyl fluorescence in the wavelength range

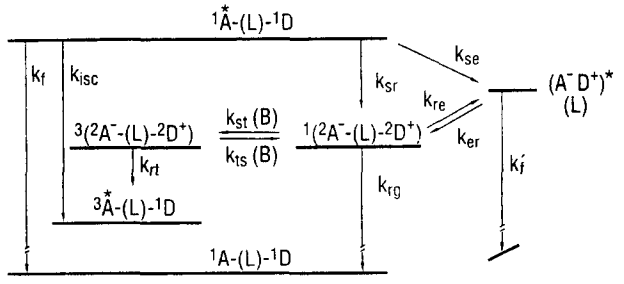

Fig. 2. General reaction scheme for intramolecular photoinduced electron transfer (PET) and return electron transfer (RET) processes of linked A–(L)–D systems in polar solvents; the linkage is designated by (L). The left-hand superscripts, e.g. in $^3(^2A^-(L)^2D^+)$, indicate that the radical anion and cation doublets (^{2}) are in an overall triplet (^{3}) spin state. Some rate constants are characterized by pairs of letters which identify the initial and final states of the reaction; singlet state (s), triplet state (t), radical ion pair (r), exciplex state (e) and ground state (g). The spin multiplicity changes in the RIPs are denoted by the magnetic-field-dependent rates $k_{st}(B)$ and $k_{ts}(B)$. Radiative transitions are denoted by k_f and k_f', and intersystem crossing by k_{isc}.

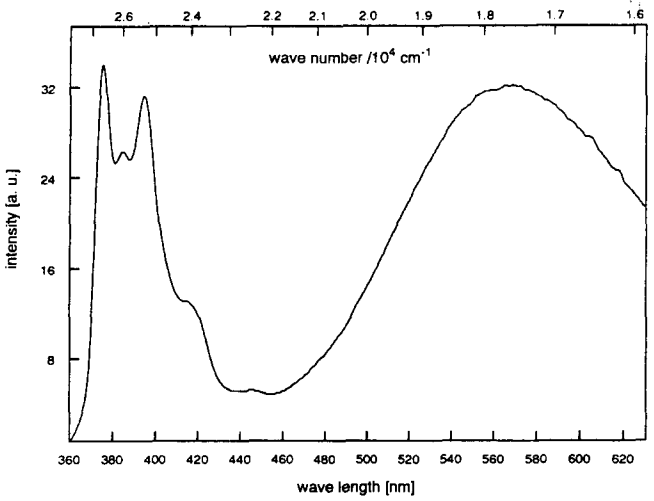

Fig. 3. Photostationary fluorescence spectrum of $2Py(Pt)_3DMA$ in acetonitrile.

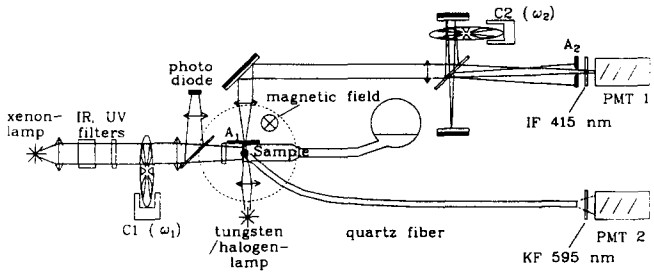

Fig. 4. Spectrometer with phase-sensitive (lock-in) detection for measurement of the magnetic-field-dependent exciplex fluorescence and triplet absorption. C1, C2, chopper with frequencies ω_1 and ω_2 respectively; A_1, A_2, apertures; IF, interference filter; KF, edge filter; PMT 1, PMT 2, photomultiplier tubes. The broken circle indicates the pole pieces of the (ESR) electromagnet.

360–480 nm and the exciplex fluorescence band with a maximum at 565 nm of compound $2Py(Pt)_3DMA$ in acetonitrile.

Adopting features of an earlier set-up [14], a new apparatus was constructed [15], allowing MFE measurements of both triplet absorption and exciplex emission (see Fig. 4). This type of instrument is advantageous if the samples are not particularly photostable. Unsatisfactory photostability (probably chain ruptures) has been encountered with peptide chains as well as with polyether and partly aromatic chains [16], in contrast with aliphatic chains. In the apparatus of Fig. 4, the light beam of a short-arc xenon lamp (Osram XBO 150W1) is chopped by a rotating sector disc with a chopping frequency ω_1 (in the range 30–200 s^{-1}). The magnetic field strength in the electron spin resonance (ESR) laboratory magnet together with the remanence-field compensation coil can be adjusted between zero and 10 kG (1 T).

2.1. Emission measurements

A quartz light guide conducts the fluorescence light from the sample to the remote photomultiplier tube (PMT 2), placed in a region without stray field from the magnet. The spectral range of interest is selected by bandpass or edge filters in front of the PMT. In the experiments described, an edge filter with transmission above 595 nm is used, which cuts off the monomer fluorescence (pyrene fluorescence). A lock-in amplifier (LIA) measures the signal which is in phase with the reference signal from the chopper blade. A second LIA receives the signal from a photodiode monitoring the intensity and possible drifts in the excitation path. The ratio of both signals is stored in a computer which also controls the sweeps through the selected range of magnetic field strengths and facilitates the graphical representation of the fluorescence intensities as a function of the magnetic field strength. By applying the chopping method, errors due to false light and lamp instabilities can be eliminated. Experiments can be carried out at low excitation intensities preserving samples for extended studies [17].

The relative exciplex fluorescence intensity I' as a function of the magnetic field strength (magnetic induction in gauss, measured with a Hall probe) is

$$\Delta\varphi/\varphi = \frac{I'(B) - I'(0)}{I'(0)} \quad (1)$$

The lower limit for the detectability of a relative exciplex fluorescence change is $\Delta\varphi/\varphi = 0.005$.

Emission decay curves were measured with the single-photon-counting method through interference filters (time resolution, 0.7 ns). Pyrenyl fluorescence signals at 377 nm were deconvoluted, allowing for the signal from the excitation pulse at 337 nm, before a function of up to three exponentials was fitted (see Eq. (3), Section 3). Picosecond lifetimes of the primary fluorescence were obtained at 408 nm by using a streak camera (Hamamatsu C1370-01) and excitation with the third harmonic from an Nd:glass laser ($\lambda = 351$ nm, $t_{FWHM} \approx 7$ ps) [18].

2.2. Absorption measurements

A tungsten/halogen lamp is placed below the pole pieces of the electromagnet. The filament is imaged through the sample near the bottom of the cuvet onto an aperture (0.6 mm × 2.5 mm) closely adjacent to the upper edge of the horizontal cuvet. The excited sample volume and measuring beam coincide well and the stray fluorescence light reaching the detector is minimized. The collimated beam is directed to the cathode of photomultiplier tube PMT 1. In order to detect the intensity of the measuring light simultaneously, an additional optical path has been introduced into the

measuring channel. A 45° beam splitter and two parallel mirrors and a chopper are inserted (see Fig. 4). The light chopped with frequency ω_2 ($\omega_2 \gg \omega_1$) (a fraction of about 10^{-4} of the total intensity) is added at the photocathode of PMT 1 to the light modulated at ω_1 which carries the absorption information of the transient species introduced by the chopped (ω_1) excitation light. If the transient is pyrene in its first excited triplet state, interference filters at 415 nm (10 nm halfwidth) are used (maximum of T_1–T_n- absorption). The number of dynodes of PMT 1 have been reduced electrically to six in order to avoid non-linearities at higher intensities of the measuring light. Two LIAs (HMS 500) of identical design handle the signals simultaneously. The first LIA receives the reference signal from chopper 1 (ω_1) and therefore measures the signal that corresponds to the absorption. The second LIA, whose reference signal comes from chopper 2, measures a signal that is proportional to the measuring light intensity which may not be constant in time. The ratio of both values is recorded. Additional corrections due to variations in the excitation intensity can be applied with a third LIA with the signal from the photodiode. In order to avoid distortions of the MFE curves due to non-first-order triplet deactivation (e.g. T–T annihilation), triplet concentrations must be kept at reasonable levels [19]. Such influences can be excluded in the present measurements.

A comparison of the performance of the instrument described above with a laser pump-and-probe set-up [20,21] yields the following advantages: it is simple and inexpensive; sensitive emission and absorption measurements are possible with the same instrument; a shorter measuring time is required to achieve comparable signal-to-noise ratios; and a lower light intensity can generally be used. Disadvantages include the considerable effort necessary to separate the fluorescence light in absorption measurements, i.e. an apparent suppression of the absorption signal due to the superposition of the 180°-phase-shifted fluorescence signal, and the consequent limitation of this method to samples with a low fluorescence emission, unless an extra calibration run is made to take care of the interfering fluorescence signal.

The samples were prepared as described elsewhere [22]. The solvents acetonitrile and acetone (Merck Uvasol, spectroscopy grade) were used as purchased, after drying over a molecular sieve (0.3 nm). Compounds were of high performance liquid chromatography (HPLC) grade.

3. Results and discussion

From the decay time of the primary fluorescence of pyrenyl, we can determine the rate constant of ET from the donor DMA to the excited acceptor pyrenyl. Assuming that ET is the predominant quenching process, we have

$$k_{ET} = \frac{1}{\tau} - \frac{1}{\tau_0} \tag{2}$$

where τ_0 is the fluorescence lifetime of the unquenched pyrenyl (e.g. methylpyrene). Table 1 shows the lifetime data and k_{ET} values obtained according to Eq. (2). Frequently, the decay curves of monomer and exciplex fluorescence were not monoexponential and had to be fitted to a sum of exponentials according to

$$I(t) = C_0 e^{-t/\tau_0} + C_1 e^{-t/\tau_1} + C_2 e^{-t/\tau_2} + \ldots, \tag{3}$$

The term with time constant τ_0 describes a slow decay process (with small prefactor), which can generally be assigned to the fluorescence from molecular fragments which are not quenched intramolecularly, and exhibit the lifetime of pyrene or methylpyrene ($\tau_0 = 190$ ns). The occurrence of shorter lifetimes, $\tau_1, \ldots, \tau_n$, from $(Pt)_3$ molecules points to different contributions to the quenching process. Although a three-exponential fit looks quite satisfactory, we propose a non-discrete distribution of lifetimes for the decay curves of the primary emission of the peptide compounds. In such cases, also applied to exciplex emission decay curves, a single survival time $\langle\tau\rangle$ [23] is used (see Table 1) which is calculated according to

$$\langle\tau\rangle = \frac{\sum_{i-1}^{n} C_i \tau_i}{\sum_{i-1}^{n} C_i} \tag{4}$$

This is the time for which equal areas are obtained under the experimental decay curve and a monoexponential decay curve with $\langle\tau\rangle$ as the decay time and ΣC_i as the pre-exponential factor.

Table 1
Fluorescence decay times of peptide- and (for comparison) alkane-linked [10,11] molecules in acetonitrile (MeCN). Electron transfer rates were calculated according to $k_{ET} = 1/\tau - 1/\tau_0$; for methylpyrene, $\tau_0 \approx 190$ ns

Molecule	τ (ns)	k_{ET} (10^9 s^{-1})	$\langle\tau_{Exc}\rangle$ (ns)
1Py(Pt)$_1$DMA	0.18	5.6	0.5
1Py(4)DMA	0.46	2.2	3.9
1Py(Pt)$_3$DMA	⟨0.54⟩[a]	1.77	15.0
2Py(Pt)$_3$DMA	⟨0.59⟩[b]	1.71	24.7
1Py(9)DMA	1.5	0.66	15.6
2Py(9)DMA	1.8	0.55	16.9
1Py(10)DMA	1.7	0.59	18.9
2Py(10)DMA	1.8	0.55	18.6

[a]Decay times between 70 ps and 2.0 ns.
[b]Decay times between 0.26 and 1.54 ns.

The times obtained reveal a clearly more effective ET with peptide chains compared with CH_2 chains. ET rates k_{ET} for comparable chain lengths ($(Pt)_1$ and $(CH_2)_4$ or $(Pt)_3$ and $(CH_2)_9$) are a factor of about three larger for peptide chains. The short components point to contributions from through-bond mechanisms, as reported previously for peptide-linked A–D systems [4,5]. Possible origins of this contribution may be found in the superexchange mechanism according to Ref. [24], or tunneling through "conducting states" of the chain as suggested by Petrov [25] for protein chains. More generally, we prefer to speak of a spacer-molecule-assisted ET (SMA-ET) as an important contribution to the quenching process. A multiexponential fluorescence decay in peptide-linked A–D systems has been described in Ref. [4]. On the other hand, the short time components could originate from a fraction of molecules preformed in close end group conformations. This explanation finds support from the higher exciplex yields of $(Pt)_3$ molecules compared with alkane-linked molecules. The intensity ratios $I'(580)/I(377)$ of exciplex fluorescence at 580 nm and fluorescence at 377 nm from quenched pyrenyl are as follows: 1Py(Pt)$_3$DMA, 12.5%; Py(10)DMA, 5.5%; 2Py(Pt)$_3$DMA, 96%; 2Py(10)DMA, 46%.

In many earlier investigations of combined A–D molecules of comparable type, where exciplex and RIP lifetimes were identical, it was concluded that exciplexes were also generated by association of RIPs in fast dynamic equilibrium with each other [10,22]; the kinetics of exciplex decay can therefore serve as a monitor for return electron transfer (RET). By measuring the absorption kinetics at 495 nm (absorption of the Py^- radical ion), this was also verified with 1Py(Pt)$_3$DMA and 2Py(Pt)$_3$DMA. Since the exciplex decays were mostly non-monoexponential, as generally also observed with polymethylene-linked compounds [10], a mean decay time $\langle\tau_{Exc}\rangle$ was determined according to Eq. (4). The time τ_1, the rise time of the signal at a wavelength near the maximum of the exciplex fluorescence band, is in all cases identical with the decay time of the primary fluorescence of pyrenyl. This illustrates that the primary excited state is the precursor which leads to the RIP and to the exciplex. The lifetimes listed in the last column of Table 1 indicate an increase in the RET rate, compared with the polymethylene chain, only for the short peptide chain; moreover, the exciplex emission of the two compounds is weak. The other compounds listed in Table 1 show exciplex lifetimes of comparable magnitude; a significant difference between the two types of chains is absent. It is remarkable that an SMA mechanism is found in the primary ET reaction, but does not seem to be effective in the RET reaction; this has also been observed experimentally in systems with spacers incorporating aromatic groups [16].

The compounds 1Py(Pt)$_3$DMA and 2Py(Pt)$_3$DMA in acetonitrile show an MFE in the exciplex fluorescence and triplet absorption, in contrast with the shorter compounds (1Py(Pt)$_1$DMA and 1Py(Pt)$_2$DMA), where an MFE is not detectable. The MFE curves obtained at the exciplex emission band are depicted in Fig. 5. They essentially show saturation-type characteristics with only a weak contribution from J-resonance-type effects [10]. The curves and the characteristic MFE values B_{min} and B_{cross} (the magnetic field strength at which an MFE curve crosses the $\Delta\varphi/\varphi=0$ line) are, in contrast with that expected for intramolecular hydrogen bonds [13], very similar to those of polymethylene-linked molecules. Results from the latter are included in Table 2 and are given in Fig. 7 for comparison. The curves from the peptide molecules of comparable extended length are shifted to somewhat smaller field strengths compared with Py(10)DMA and 2Py(10)DMA. This corresponds to the effect of an A–D distance distribution displaced to somewhat larger separations. Monte-Carlo calculations led to differences in the average separations between the isomers Py(9)DMA and 2Py(9)DMA, as well as between Py(10)DMA and 2Py(10)DMA [11]. Typical differences were 0.6–0.8 Å for identical chain lengths. If these results are applicable to peptide-linked molecules, the slight shift of the MFE curve can be explained by a shift in the pair distribution function of only 0.2–0.4 Å towards longer distances. However, such an interpolation can only be accepted provided that other parameters, such as the molecular dynamics, distance dependence of the exchange interaction and rigidity of the chain, are identical. The same MFE curve may also result from a different combination of these parameter values.

As expected, the MFE in the triplet absorption with an inverted curve shape (see Fig. 6) shows the same

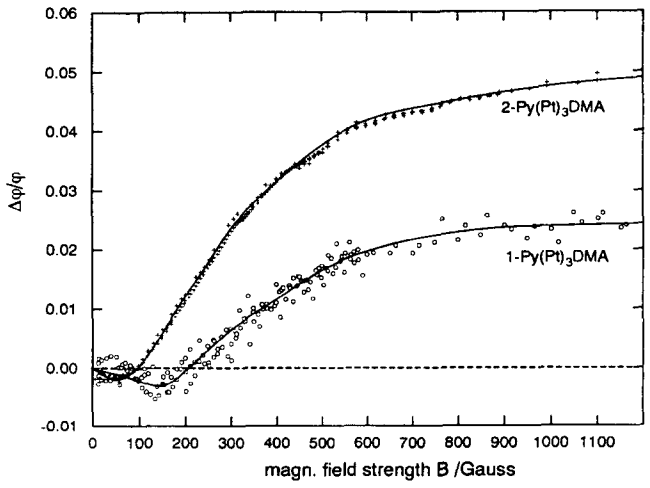

Fig. 5. Magnetic field dependence of exciplex emission of 1Py(Pt)$_3$DMA and 2Py(Pt)$_3$DMA in acetonitrile. Full lines were obtained by spline approximation of the data points.

Table 2
Characteristics of MFE spectra (for definitions, see text) of peptide- and (for comparison) alkane-linked molecules in the solvents acetonitrile (MeCN) and acetone

Molecule	Solvent	B_{max} (G)	B_{cross} (G)	$\Delta\varphi/\varphi\|_{max}$ (%)	$\Delta\varphi/\varphi\|_{sat}$ (%)	R_{max} (%)	R_{sat} (%)
1Py(Pt)$_3$DMA	MeCN	150	205	−0.3	2.5	−2	22
1Py(Pt)$_3$DMA	Acetone	160	250	−0.6	4.8	−3	11
2Py(Pt)$_3$DMA	MeCN	50	97	−0.15	5.0	−1	18
1Py(9)DMA	MeCN	280	486	−4.9	5.5	−29	36
2Py(9)DMA	MeCN	106	169	−2.0	18		
1Py(10)DMA	MeCN	100	167	−2.3	19	5.5	39
1Py(10)DMA	Acetone	90	150	−1.2	28	3.5	25
2Py(10)DMA	MeCN	46	67	−0.8	33		

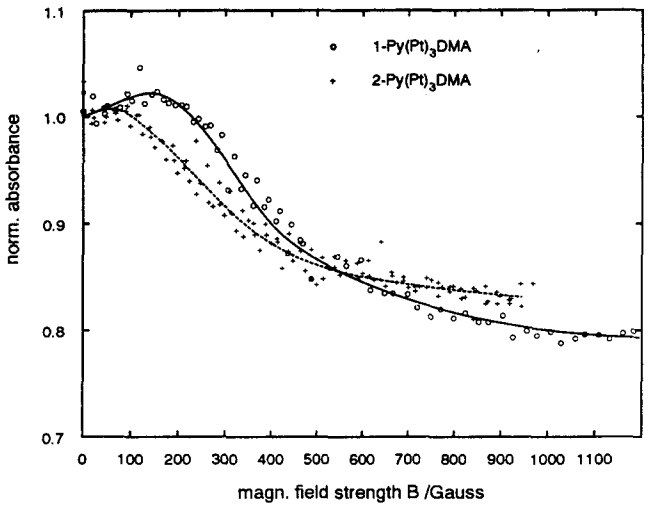

Fig. 6. Magnetic field dependence of pyrenyl triplet absorbance of 1Py(Pt)$_3$DMA and 2Py(Pt)$_3$DMA in acetonitrile.

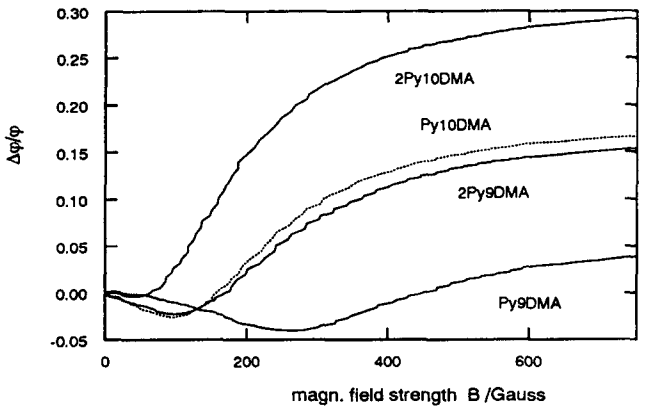

Fig. 7. MFE curves of the exciplex emission of 1Py(9)DMA, 2Py(9)DMA, 1Py(10)DMA and 2Py(10)DMA.

characteristic B values as the MFE of the exciplex fluorescence (see Ref. [10]). The magnitude of the effect (R value in Table 2; $R_{sat} = 1 - \phi_T(B = \infty)/\phi_T(B = 0)$, $R_{max} = 1 - \phi_T(B = B_{max}/\phi_T(B = 0))$ is considerably larger in absorption. This is not a novel observation; the increasing discrepancy with decreasing chain length between $\Delta\varphi/\varphi$ and R values obtained with the two detection methods (exciplex emission and triplet absorption) is also evident in the polymethylene-linked compounds. The reason for this is that, with decreasing chain length, an increasing fraction of molecules, within the RIP lifetime, do not reach intrapair distance ranges leading to a sufficiently low exchange interaction J to allow hfc-induced intersystem crossing, $^1(^2A^- - ^2D^+) \rightarrow {}^3(^2A^- - ^2D^+)$, followed by recombination $^3(^2A^- - ^2D^+) \rightarrow {}^3A^* - D$ (see Fig. 2). The reduced spin conversion efficiency leads to a smaller absorbance in the MFE detection of the triplet yield, but with the relative MFE value (R value) remaining the same. However, in emission this leads to an increasing fraction of exciplexes, generated (independent of the magnetic field) from RIPs, which have never reached the "magnetic-field-sensitive" intrapair distance range.

The characteristic field strengths in Table 2, B_{max} and B_{cross}, are average values obtained from emission and absorption measurements; because of the given signal-to-noise ratio, the total uncertainty is of the order of 10 G.

A possible influence of weak intermolecular hydrogen bonds on peptide chain conformations has been reported in Ref. [13]. Putative intramolecular hydrogen bonds (between CO and NH of the same amino acid residue) in an oligopeptide chain of the type $(Pt)_3$ might lead to an extended conformation in the solvent acetonitrile (which is inert towards hydrogen bonding with the peptide function). On the other hand, in solvents with hydrogen-accepting properties, such as acetone [26,27], the intramolecular hydrogen bond could be destroyed by intermolecular hydrogen bonds between the solvent and the peptide chain. If this were the case with acetone, we would expect a shift of the B_{max} and B_{cross} values towards higher field strengths and also a smaller MFE. The difference between the viscosities of acetonitrile and acetone is small ($\eta_{MeCN} = 0.36$ mPa s, $\eta_{Acetone} = 0.32$ mPa s) and would not lead to a significant shift [10,28]. From our present studies (with oligopeptide chains), we were unable to draw inferences with respect to

molecular dynamics which are comparable with those of Ref. [13]. The differences between the MFE curves obtained in acetonitrile and acetone can simply be attributed to the different polarities of the solvents ($\epsilon_{MeCN} = 37.5$, $\epsilon_{Acetone} = 20.7$). The consequences of varying solvent polarity on the MFE of recombining unlinked and chain-linked RIPs have been extensively studied and will be reported elsewhere [29]. From the similarity between the MFE curves obtained with peptide-linked and alkane-linked molecules, we conclude that the intramolecular mobility of the two sets of molecules is comparable in both solvents. Therefore intramolecular hydrogen bonds seem to be of minor significance to the intramolecular dynamics, at least for the peptide chain $(Pt)_3$ consisting of three glycine groups. MFE experiments with molecules containing different numbers of glycine/proline groups are in progress.

From the MFE and RIP lifetimes obtained with $(Pt)_3$ systems, no indications of a through-bond mechanism, assisting the return electron transfer or enhancing the spin exchange interaction, were found. This is in line with the results obtained with compounds incorporating phenyl groups in an aliphatic chain. There, we also found SMA-ET (i.e. probably a through-bond mechanism for the primary charge separation), but the return electron transfer was insignificantly influenced or not influenced by such a mechanism [16].

Acknowledgement

We thank B. Frederichs and H. Meyer for technical assistance.

References

[1] S.S. Isied, M.Y. Ogawa and J.F. Wishart, *Chem. Rev., 92* (1992) 381, and references cited therein.
[2] S.S. Isied and A. Vassilian, *J. Am. Chem. Soc., 106* (1984) 1726.
[3] S.S. Isied, Electron transfer in inorganic, organic and biological systems, in J.R. Bolton, N. Mataga and G. McLendon (eds.), *Advances in Chemistry,* Vol. 228, ACS, CSC, Washington, Ottawa, 1991, p. 229.
[4] K.S. Schanze and K. Sauer, *J. Am. Chem. Soc., 110* (1988) 1180.
[5] J.Y. Liu, J.A. Schmidt and J.R. Bolton, *J. Phys. Chem., 95* (1991) 6924.
[6] D.N. Beratan and J.N. Onuchic, Electron transfer in inorganic, organic and biological systems, in J.R. Bolton, N. Mataga and G. McLendon (eds.), *Advances in Chemistry,* Vol. 228, ACS, CSC, Washington, Ottawa, 1991, p. 71.
[7] J.R. Bolton, J.A. Schmidt, T.-F. Ho, J. Liu, K.J. Roach, A.C. Weedon, M. Archer, J.H. Wilford and V.P. Gadzekpo, Electron transfer in inorganic, organic and biological systems, in J.R. Bolton, N. Mataga and G. McLendon (eds.), *Advances in Chemistry,* Vol. 228, ACS, CSC, Washington, Ottawa, 1991, p. 117.
[8] Y. Inai, M. Sisido and Y. Imanishi, *J. Phys. Chem., 95* (1991) 3847.
[9] U.E. Steiner and H.-J. Wolff, in J. Rabek (ed.), *Photochemistry and Photophysics,* Vol. IV, CRC Press, Boca Raton, FL, 1991, Chapter 1, p. 1.
[10] H. Staerk, H.G. Busmann, W. Kühnle and R. Treichel, *J. Phys. Chem., 95* (1991) 1907.
[11] U. Werner and H. Staerk, *J. Phys. Chem., 97* (1993) 9274.
[12] R. Bittl and K. Schulten, *J. Chem. Phys., 90* (1989) 1794.
[13] F. Ruttens, R. Goedeweek, F. Lopez-Arbeloa and F.C. De Schryver, *Photochem. Photobiol., 42* (1985) 341.
[14] H. Staerk, *J. Lumin., 11* (1976) 413.
[15] U. Werner, *Dissertation,* University of Göttingen, 1993.
[16] H. Staerk, W. Kühnle, A. Weller and U. Werner, *Z. Phys. Chem. (Wiesbaden), H.G.-Wagner-Festschrift,* 1994.
[17] U. Werner, W. Kühnle and H. Staerk, *J. Phys. Chem., 97* (1993) 9280.
[18] A. Wiessner and H. Staerk, *Rev. Sci. Instrum., 64* (1993) 3430.
[19] N.L. Lavrik, U. Werner, Yu.N. Molin and H. Staerk, *J. Chem. Phys., 99* (1993) 9304.
[20] R. Treichel, *Dissertation,* University of Göttingen, 1985.
[21] R. Treichel, H. Staerk and A. Weller, *Appl. Phys. B, 31* (1983) 15.
[22] H. Staerk, W. Kühnle, R. Treichel and A. Weller, *Chem. Phys. Lett., 118* (1985) 19.
[23] R.A. Marcus and H. Sumi, *J. Electroanal. Chem., 59* (1986) 204.
[24] S. Larsson, *J. Am. Chem. Soc., 103* (1981) 4034.
[25] E.G. Petrov, *Int. J. Quantum Chem., XVI* (1979) 133.
[26] C. Reichardt, *Solvents and Solvent Effects in Organic Chemistry,* VCH, Weinheim, 1988.
[27] S.N. Vinogradov and R.H. Linnell, *Hydrogen Bonding,* Van Nostrand Reinhold, New York, 1972.
[28] H.-G. Busmann, H. Staerk and A. Weller, *J. Chem. Phys., 91* (1989) 4098.
[29] U. Werner and H. Staerk, *J. Phys. Chem.,* submitted.